Finite Element Analysis and Experiments for Predicting Fatigue and Rolling Contact Fatigue Behavior of Spur Gears

Sergio Baragetti[1*]

[1] Department of Management, Information and Production Engineering, University of Bergamo, Viale Marconi 5, Dalmine 24044, Italy
[*] Corresponding author, e-mail: sergio.baragetti@unibg.it

Abstract

This paper presents the Finite Element (FE) analyses carried out with the aim to predict the tooth root fatigue and Rolling Contact Fatigue (RCF) behavior of spur gears, in terms of crack propagation maximum number of cycles. The combination of different materials, i.e. steel and titanium, and surface treatments, i.e. case-hardening and application of surface layers by Physical Vapor Deposition (PVD), are investigated. The residual stresses induced by the deposition of the coating are modelled. The stress intensity is described by linear elastic relations based on the crack tip opening displacement and the crack propagation in the case-hardened spur gears is described with the help of mathematical models. Experiments are carried out to evaluate tooth damage under RCF for different treated gears. The best solutions in terms of bulk material – treatment combination among the ones investigated are identified, also highlighting innovative possibilities which can guarantee appreciable performance.

Keywords

spur gears, PVD, fracture mechanics, FEM, experiments

1 Introduction

Innovation in the field of spur gears is challenging, in particular for high-strength automotive components, where high mechanical performance is required in terms of wear resistance, contact fatigue and fatigue behavior. The material treatments can considerably alter the mechanical and tribological behavior of the substrate and therefore lead to a possible improvement in the performance of the spur gears. To date, case-hardened steel gears are preferred, since case-hardening guarantees an increase of surface hardness which improves the fatigue strength and the surface properties. Tribological properties and resistance to corrosion and contact fatigue can be improved by adopting PVD thin hard coatings, which guarantee a significant increase in hardness of the external surface. PVD films are often adopted for cutting tools. For example, the deposition of a CrN PVD coating has been shown to enhance the fatigue strength of H11 tool steel grade [1]. These coatings are also deposited on aviation gas turbines, according to the paper [2] on the application of coatings on superalloy airfoils. Other applications include biomedical implants as reported in a review on the use of DLC coatings [3], automotive components [4] and methanol fuel cells [5].

In detail, Bobzin et al. [4] analyzed the WC/C and CrAlN coatings with various lubricants and found that the wettability of the surface and the friction behavior depend on the adhesion energy. Zellner and Chen [5] instead studied the changes in the composition of the WC and W_2C films and their stability in order to evaluate their protective action. The deposition of these films on mechanical components can therefore increase their fatigue strength, under suitable parameters of the coating deposition process and surface preparation. The parameter which most influences fatigue strength is the residual stress induced by the coating deposition, which must be highly compressive [6]. It was found that CrN coating improves fatigue strength of steel but not of aluminum. The Authors suggested that the latter behavior is a consequence of a significant aging of the aluminum alloy. The process temperature is another critical variable for fatigue strength since it can negatively influence the substrate microstructure, mainly in the case of alloys with low aging temperatures, as observed for instance in [7] for a ZrN coating on 7075-T6 aluminum alloy. Therefore, low temperature coatings should be preferred, particularly if deposited on light alloys, as confirmed in a study on the

contribution of type of coating and deposition temperature on 7075-T6 aluminum alloy [8]. The deposition of DLC coatings has been found to globally reduce the fatigue strength of 7075-T6 aluminum alloy within the number of cycles range 200,000–10,000,000 [9–12]. Another study which testifies to the doubtful contribution of PVD coatings on fatigue strength, better RCF strength, is presented in [13], where a more uniform damage-load diagram was obtained for uncoated spur gears compared to the coated components. However, it has to be stressed that the loads applied in this study were high and for this reason could have caused the coating to fracture. In addition, adequate polishing is required, i.e. the average roughness must be less than 0.1 μm, since the presence of flaws combined with the steep residual stress gradient can easily lead to crack nucleation and delamination of the coating [8], defeating any attempt to improve the mechanical properties of the machine component. The choice of good parameters, e.g. substrate-coating combination and thermal load applied, can significantly improve the fatigue strength of the machine components, in particular for low stress levels at long fatigue lives [14, 15].

PVD films can be applied in new design strategies for high performance spur gears. For example, Kumar and Arul [16] experimentally found that a cuprous oxide can improve the overall strength of a mild steel spur gear. An experimental campaign to find the best coating-substrate combination can be expensive and time consuming. In order to help the mechanical designer save time, this paper describes FE models for fatigue and RCF which allow the designer to foresee the propagation of a crack located in the tooth contact area and the consequent number of cycles needed to reach certain crack lengths for fatigue and RCF of spur gears, considering different substrate-coating combinations and including the effects of a possible heat treatment [17–19]. The spur gears of a Ducati 1098R competition motorcycle were analyzed, considering different materials, treatments and coatings. RCF experimental testing on case-hardened uncoated and WC/C coated spur gears is shown in [19]. FE models for coated Ti6Al4V spur gears were also built to study the fatigue performance guaranteed by this solution. Titanium alloys are indeed critical for the manufacture of spur gears because of their poor shear strength and tribological properties, and an effective PVD coating could lead to a possible application of these alloys for high strength-to-weight spur gears. Spur gears are fundamental components in transmission systems and for this reason a light weight

should be preferred for them. Saleem et al. [20] proposed for example a composite spur gear made of aluminum and organic compound and Czinege [21] applied the Ashby model to optimize the mass of the gears. Polymer gears can be useful for obtaining low weight transmission systems for aerospace and automotive applications and for this reason Zhang et al. [22] studied 3D printed nylon gears.

In this paper, the best combinations of bulk material – treatment for tooth root fatigue and RCF among the ones investigated were identified. Innovative solutions with appreciable performance are described.

2 Materials and methods
2.1 FE analysis for tooth root fatigue
A comprehensive procedure to analyze the propagation of a surface crack located at the base of the tooth in spur gears is shown in [17]. The studied spur gears are of a Ducati 1098R competition motorcycle and made of 15NiCr13 steel or Ti6Al4V titanium. A detailed characterization of Ti6Al4V under static load in different environments is presented in [23]. The properties of the materials and of the coatings investigated in this analysis are shown in Table 1 [17], where E is Young's modulus, v Poisson's ratio, YS the yield tensile strength and UTS the ultimate tensile strength. The same surface hardness value was adopted for CrN and TiN coatings as the deposition processes are similar [24]. A surface compressive residual stress $\sigma_{res} = -2,500$ MPa was imposed on both coatings, according to the measurements conducted in [6].

The 3D FE model of Fig. 1 [17] was created to foresee the number of cycles for fatigue crack propagation. Both the pinion and the lead gear were modeled to identify the load-induced stress distribution at the base of the tooth. A semi elliptical crack with a depth of 5 μm and a width of 20 μm, normal to the surface, was modelled in the area where maximum bending stress is reached. A mesh of linear tetrahedral and hexahedral elements was adopted. The mesh of the whole model and the detail in the engagement area

Table 1 Material properties, adapted from [17]

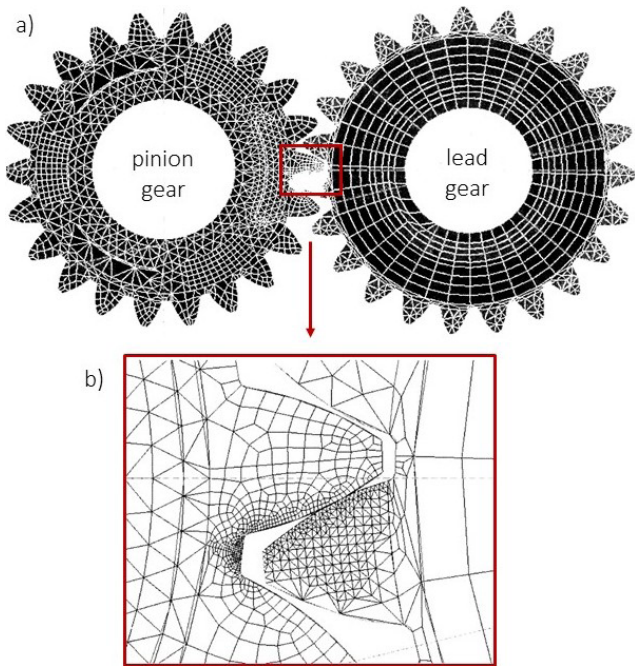| Material	15NiCr13	Ti6Al4V	CrN	TiN
Condition	Case-hardened	Annealed	PVD coating	PVD coating
Hardness [HV]	300	350	2,680	2,680
E [GPa]	206	113	303	600
v	0.28	0.34	0.20	0.25
YS [MPa]	883	880	N/A	N/A
UTS [MPa]	1,128	950	N/A	N/A
σ_{res} [MPa]	0	0	−2,500	−2,500

Fig. 1 3D FE model of the matching spur gears for tooth root fatigue: (a) whole model; (b) detail in the engagement area, adapted from [17]

are shown in Fig. 1 (a) and (b), respectively. Due to the small size of the crack, it was impossible to have an appropriate mesh refinement at the crack tip. For this reason, a sub-modeling technique was adopted. Fig. 2 [17] summarizes the technique: Fig. 2 (a) shows the area where the flaw was positioned, Fig. 2 (b) the refinement of the mesh in the created sub-model, Fig. 2 (c) a general stress distribution in the sub-model, Fig. 2 (d) is a detail, in Fig. 2 (e) the dimensions of the cracks are indicated and in Fig. 2 (f) a general stress state at the crack front is shown.

The compressive stress field induced by the coating deposition, or rather the compressive stress on the surface of the component, is related to crack propagation [17]. An adequate self-equilibrated residual stress field must be defined in the model, according to [6]. The values of surface residual stress adopted in the model for the CrN PVD coating on steel spur gears and the TiN PVD coating on titanium are shown in Table 1. The residual stress distribution is characterized by a steep gradient in the coating and in the outer region of the substrate. As seen in [6], the
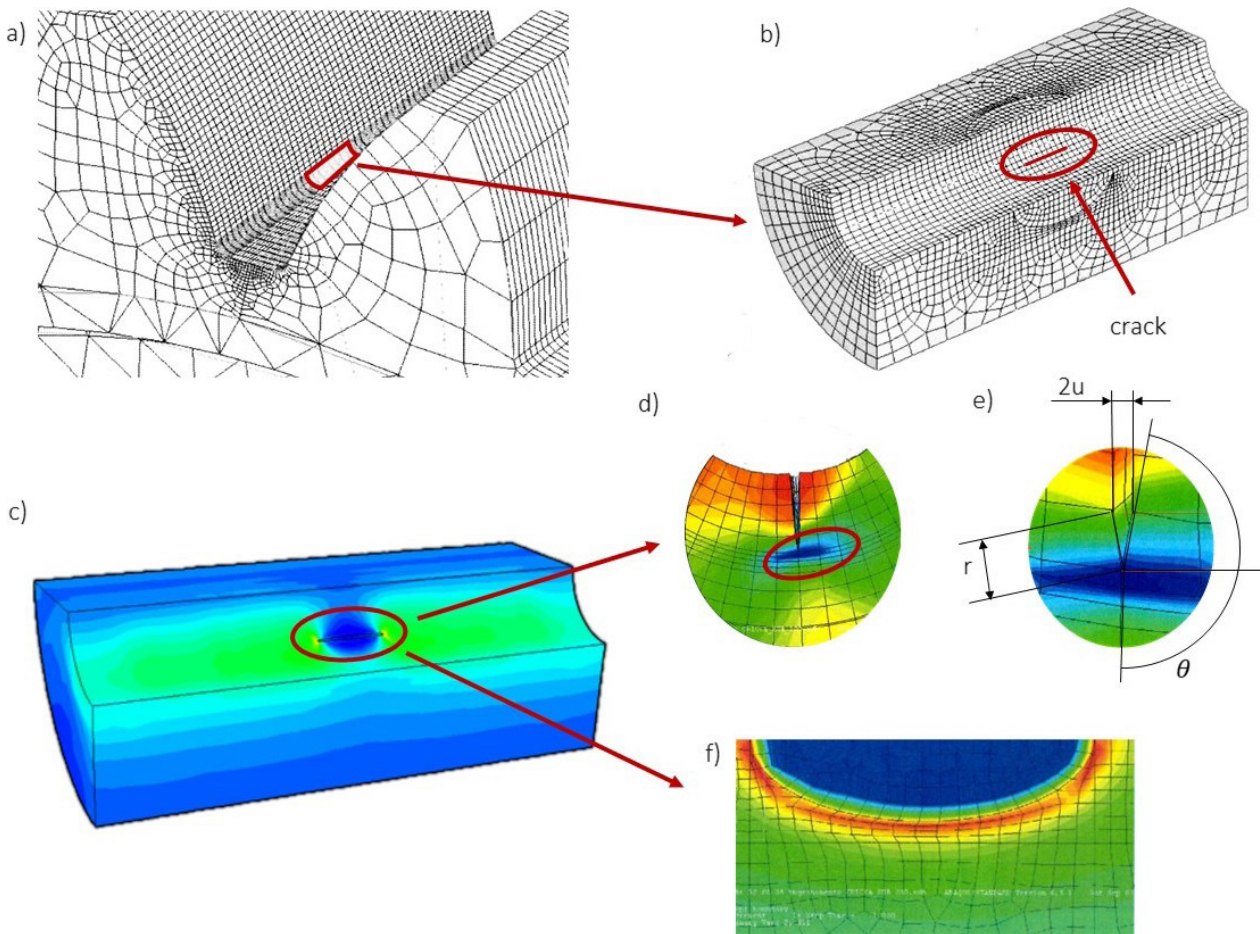

Fig. 2 Sub-modelling technique for the FE analysis for tooth root fatigue: (a) area where the flaw was positioned; (b) refinement of the mesh in the sub-model; (c) general stress distribution in the sub-model; (d) detail at the crack tip; (e) size of the crack; (f) general stress state at the crack front, adapted from [17]

residual stress field was introduced by generating an adequate temperature field. In order to prevent the elements in the proximity of the crack from overlapping as a consequence of the compression state induced by the coating deposition, a contact interaction was implemented.

After the introduction of the residual stresses, it is necessary to determine the stress intensity factor K_I, since fatigue failure mode I is preeminent in a tooth root. The stress intensity factor can be calculated with the Irwin elastic model, presented in [25] and described by Eq. (1):

$$K_I = 2 \times E / (1 + v) \times \sqrt{2\pi/r} \times u / f(\theta), \tag{1}$$

where u indicates the half crack tip opening displacement and $f(\theta)$ is defined by Eq. (2):

$$f(\theta) = (2\chi + 1)\sin(\theta/2) - \sin(3\theta/2) \tag{2}$$

with $\chi = 3 - 4v$ for plane strain state and $\chi = (3 - v)/(1 + v)$ for plane stress state. For the other parameters it is recommended to refer to Fig. 2 (e).

Equations (1) and (2) provide a linear-elastic stress distribution around the crack tip, assuming a small plasticization in this region. This small-scale yielding condition can be assumed for alloys with high yield strength [25]. Therefore, a linear-elastic material was implemented in the FE model.

The stress intensity range is calculated by considering the effect of the residual stresses as $\Delta K_{app} = K_{max} - K_{res}$, where K_{max} is the maximum value of stress intensity factor and K_{res} is the stress intensity factor due to residual stresses. This model can be applied if no delamination occurs between the coating and the bulk material. The threshold stress intensity factor range for crack propagation must be assessed by adopting the literature models developed for the microfracture mechanics regime [26–29]. The model specially designed in [30] for case-hardened spur gears was used for the crack propagation from 5 μm to 25 μm, 50 μm, 100 μm and 200 μm. According to it, the crack propagation rate da/dN is defined by Eq. (3) for $\Delta K_{th} \leq \Delta K \leq K_c$ and Eq. (4) for $K_c < \Delta K < K_{Ic}$:

$$da/dN = C/(1 - \rho^n)(\Delta K^n - \Delta K_{th}^n) \tag{3}$$

$$da/dN = C/(1 - \rho^n)(\Delta K^n K_{Ic}^n)/(K_{Ic}^n - \Delta K^n), \tag{4}$$

where a is the crack depth and N the number of cycles, ΔK the stress intensity factor range, ΔK_{th} the threshold stress intensity factor range and K_{Ic} the fracture toughness. The parameters ρ and K_c are defined in Eq. (5):

$$\rho = \Delta K_{th}/K_{Ic} \quad K_C = (\Delta K_{th} K_{IC})^{0.5}. \tag{5}$$

The parameters ΔK_{th}, K_{Ic}, n and C depend on the microhardness distribution along the gear thickness, which can be altered by the deposition of a coating and by case-hardening, according to Eqs. (6)–(9):

$$\Delta K_{th} = 2.45 + 3.41 \times 10^{-3} H \tag{6}$$

$$K_{Ic} = 141 - 1.64 \times 10^{-1} H \tag{7}$$

$$n = 4.31 - 8.66 \times 10^{-3} H + 1.17 \times 10^{-5} H^2 \tag{8}$$

$$\log(C) = -10.0 + 1.09 \times 10^{-2} H - 1.40 \times 10^{-5} H^2, \tag{9}$$

where the parameter H is related to the material hardness at different material depths, as indicated in Eq. (10):

$$H = (H_2 - H_3)\exp\left[-A(d^* - d_2)^2\right] + H_3 \tag{10}$$

where A can be determined as indicated in Eq. (11) for $d^* \leq d_2$ and Eq. (12) for $d^* > d_2$:

$$A = -1/d_2^2 \times \ln\left((H_1 - H_3)/(H_2 - H_3)\right) \tag{11}$$

$$A = -1/(d_c - d_2)^2 \times \ln\left((550 - H_3)/(H_2 - H_3)\right), \tag{12}$$

where d^* is the depth from the surface, d_2 is the depth of the maximum hardness, d_c is the thickness of the coating. H_1, H_2 and H_3 are respectively the surface Vickers hardness, the maximum hardness and the core hardness. The values for the described analysis are shown in Table 2 [17].

The integration of Eqs. (3) and (4) provides the number of cycles needed to reach a certain crack depth. The obtained results are useful for comparing the performances of the various combinations bulk material – treatment investigated in this analysis.

2.2 FEM analysis for RCF
Another source of failure for spur gears is certainly represented by RCF. In [18] and [19] a model to foresee crack

Table 2 Material hardness values needed for H calculation, adapted from [17]

Material	15NiCr13	15NiCr13	Ti6Al4V	Ti6Al4V
Condition	Case-hardened	CrN coated	Annealed	TiN coated
H_1 [HV]	720	2,680	350	2,680
H_2 [HV]	760	2,686	350	2,686
H_3 [HV]	300	300	350	350
d_2 [mm]	0.2	0.0005	N/A	0.0005
Depth of interface hardness [mm]	0.5	0.005	N/A	0.005

growth and tooth spallation is described. Due to the high thickness of the gears, a 2D plane strain model containing the pinion and the lead gear was created. The rotation of the gears was simulated starting from the initial tooth pair engagement. The gears were constrained to their axis by coupling-kinematic interaction. The pinion was left unconstrained, and loaded with a torque ranging from 244 Nm, which was the maximum value of service torque, to 300 Nm, which corresponds to 1.2 times the service load in order to consider overloading condition. The lead gear received a rotation against the torque direction, to completely model the contact between the two teeth.

Because of the difficulties in refining the mesh near the crack tip, the sub-modeling technique was also adopted in this case of RCF analysis, as shown in Fig. 3 [19]. The residual stress distribution induced by the deposition process of the coating, which is a WC/C PVD coating in this study, was modeled by imposing a pre-stress condition along the tooth flank tangential direction into appropriate solid partitions. The material was pre-cracked in a direction parallel to the tooth surface, ensuring an initial crack length of 5 μm. The base material was modeled by plane strain quadrilateral four-node bilinear elements and the coating by two-node, two-dimensional linear truss elements. Linear elastic materials were implemented. Contact interactions were defined between the tooth profiles and the flanks of the crack to avoid overlapping. The coefficients of friction implemented in the model are 0.1 and 0.3 for steel and titanium respectively. The details of the global mesh, the sub-model and the initial crack are shown respectively in Fig. 3 (a)–(c). Table 1 summarizes the mechanical properties of the Ti6Al4V alloy. The mechanical properties of the 16NiCr11 steel adopted are: $v = 0.3$, $YS = 785$ MPa and $UTS = 1,030–1,280$ MPa. The parameters needed to rebuild the hardness distribution induced by case-hardening and WC/C deposition are

shown in Table 3 [19]. The propagation model used for RCF is again the one presented in [30].

2.3 Experimental RCF tests
The RCF tests were conducted with the specifically designed testing equipment shown in Fig. 4 [19]. The components of the test rig are indicated in Fig. 4 (a). The testing torque was applied by transforming the axial load, given by a Galdabini 250 kN universal axial testing machine, with a leverage system, as shown in Fig. 4 (b). The two gears to be tested were mounted on the two shafts of the test rig. The driven shaft was constrained by a braking system, needed to avoid parasite bending stresses, which could cause overloading. The relative movement of the matching gears was made possible mainly by the torsion of the moving shaft. The amount of rotation was defined by setting the longitudinal position of the braking system along the shaft. Various tests were carried out on case-hardened uncoated and WC/C coated steel gears, in dry and lubricated conditions. The final tooth shape was determined with a profilometer with the equipment shown in Fig. 5 (a). The total volume removed and the maximum depth of damage were obtained by comparing the profile of the damaged tooth with the original profile, Fig. 5 (b) [19].

3 Results
3.1 FE analysis for tooth root fatigue
Five different crack propagation depths were studied for the FE analysis concerning the tooth root fatigue: 5, 25, 50, 100 and 200 μm. Four base material – treatment combinations were investigated: uncoated non-case-hardened steel, uncoated case-hardened steel, coated non-case-hardened steel, coated titanium. The results are shown in Table 4 [17]. Fig. 6 shows the stress field near the crack for the uncoated (Fig. 6 (a)–(e)) and coated (Fig. 6 (f)–(h)) non-case-hardened steel gears for different crack depths [17].
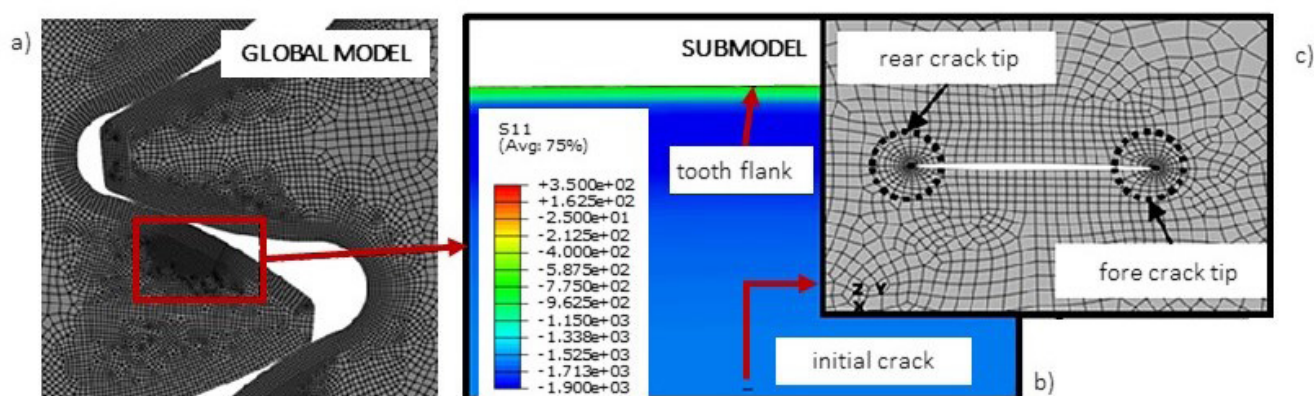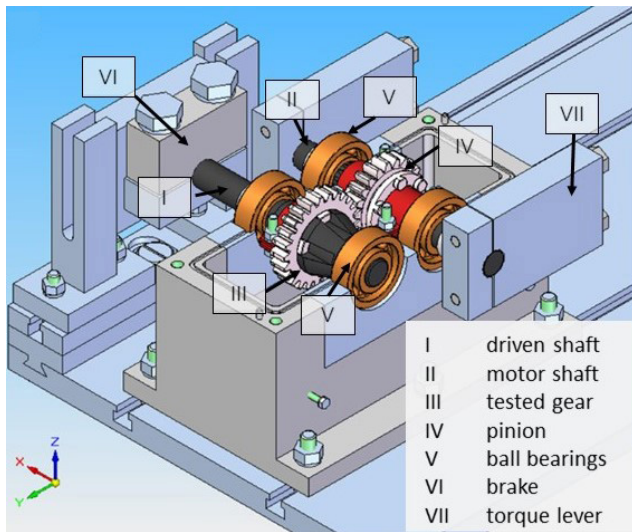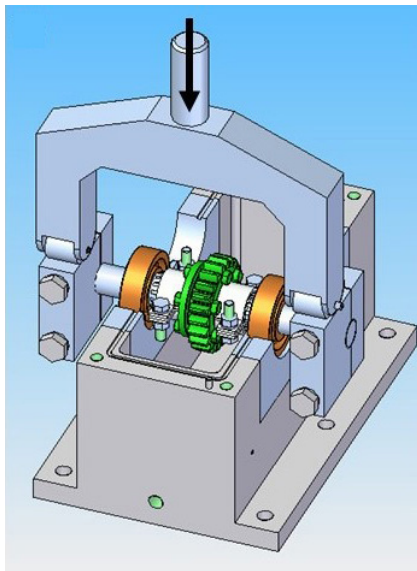

Fig. 3 FEM analysis for RCF: (a) global model; (b) sub-model; (c) detail of the initial mesh in the crack region, adapted from [19]

Table 3 Materials hardness distributions for H calculation, adapted from [19]

Material	16NiCr11	16NiCr11/Ti6Al4V
Condition	Case-hardened	WC/C coated
H_1 [HV]	720	1,200
H_2 [HV]	760	1,206
H_3 [HV]	300	300
d_2 [mm]	0.2	0.0015
Treatment thickness [mm]	0.5	0.003

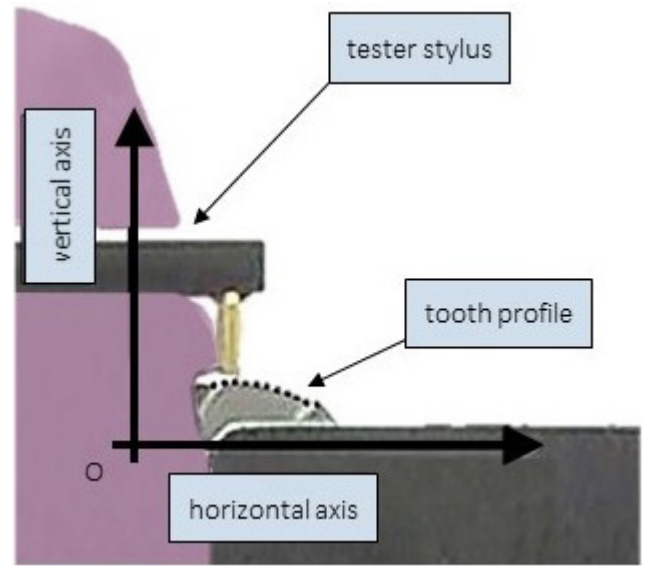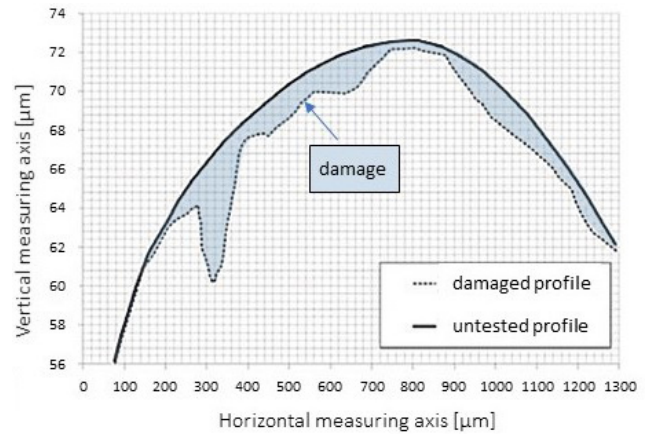| I	driven shaft
II	motor shaft
III	tested gear
IV	pinion
V	ball bearings
VI	brake
VII	torque lever

(a)

(b)

Fig. 4 Experimental RCF tests: (a) components of the test rig; (b) load application, adapted from [19]

For the latter case, only the stress distributions for crack depths greater than or equal to 50 μm are shown, since the first crack opening was detected at 100 μm.

(a)

(b)

Fig. 5 RCF tests: (a) equipment for the measurement of the tooth profile; (b) comparison between the profile of the untested and damaged gear, adapted from [19]

Table 4 Tooth root fatigue: number of cycles to reach a 200 μm crack depth, with intermediate stages, adapted from [17]

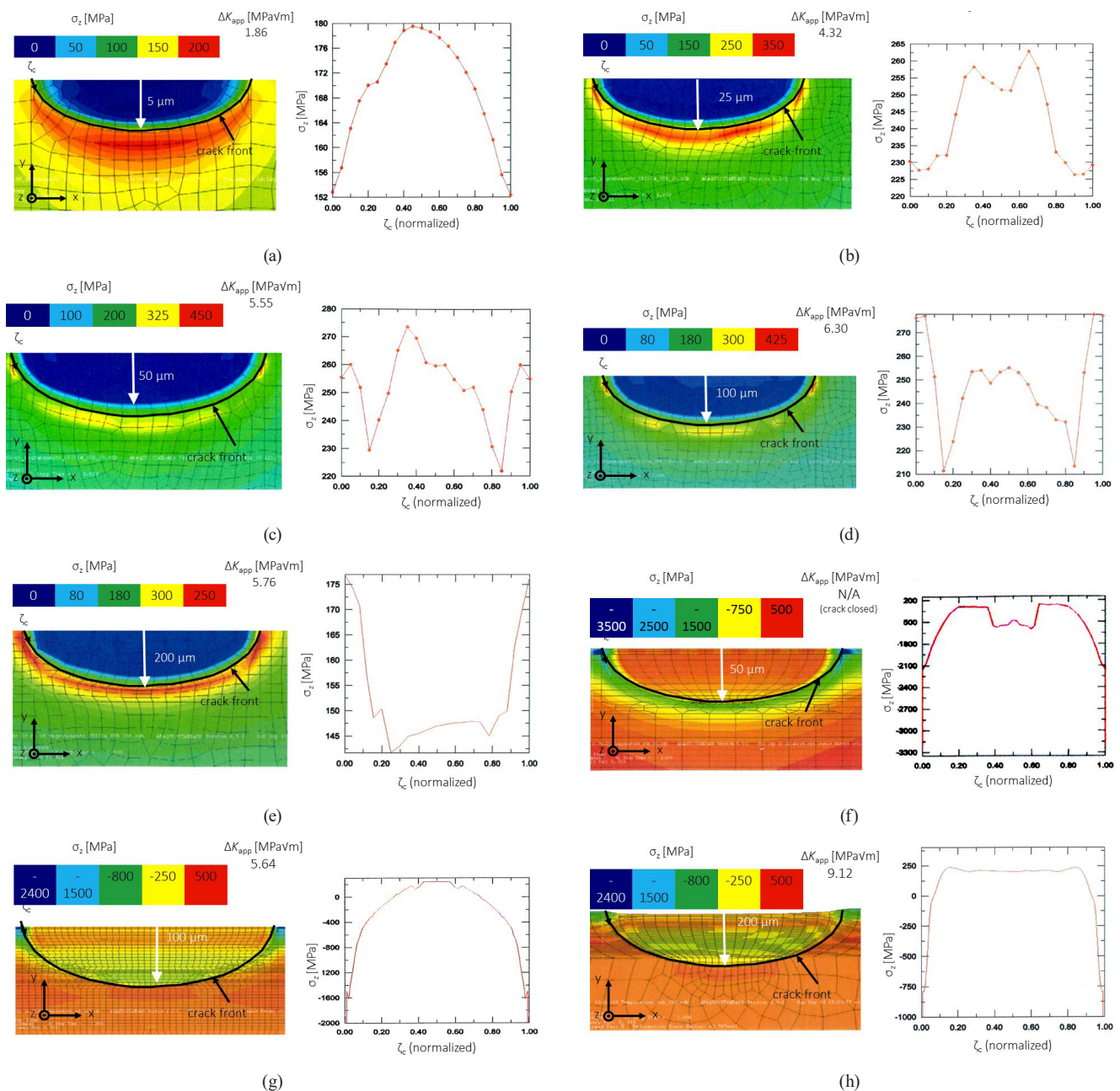| Crack depth [μm]	5–25	25–50	50–100	100–200	Fatigue life
Uncoated, non-case-hardened steel	-	60,278 cycles	86,254 cycles	106,969 cycles	253,500 cycles
Uncoated, case-hardened steel	-	-	-	-	-
Coated, non-case-hardened steel	-	-	49,976 cycles	104,184 cycles	154,160 cycles
Coated titanium	-	-	-	432,220 cycles	432,220 cycles

Fig. 6 Stress field and stress intensity factor near the crack: uncoated non-case-hardened steel (a) 5 µm; (b) 25 µm; (c) 50 µm; (d) 100 µm; (e) 200 µm; coated steel (f) 50 µm; (g) 100 µm; (h) 200 µm, adapted from [17]

3.2 FEM analysis for RCF

As regards the RCF FE analysis, simulations were run on case-hardened and WC/C coated steel and Ti6Al4V WC/C coated spur gears. For an applied torque of 244 Nm, corresponding to the service condition, no propagation was detected for a crack depth of less than 185 µm for steel gears and 265 µm for those in titanium, as found in [31]. The crack propagated under Mode II loading, at an angle of about 70° with respect to the initial direction, during the earlier propagation stages, while Mode II prevailed later. The same material – treatment combinations were studied for an applied torque of 300 Nm and an initial flaw of 5 µm.

The results are presented in Table 5 [18]. The final stress distributions are shown in Fig. 7. In detail, Fig. 7 (a) shows the final stage of crack propagation for the case-hardened steel gear, Fig. 7 (b) for the coated steel gear and Fig. 7 (c) for the coated titanium gear [18].

3.3 Experimental RCF tests

Case-hardened steel and WC/C coated steel spur gears were tested with a load ratio $R = 0.1$, at a frequency $f = 1$ Hz, with a torque of 244 Nm and in lubricated conditions, guaranteed by a F40 racing oil, for 100,000 and 150,000 cycles. The results in terms of damaged area cross

Table 5 FEM analysis for RCF: number of cycles to spallation for a torque of 300 Nm and initial crack length of 5 μm, adapted from [18]
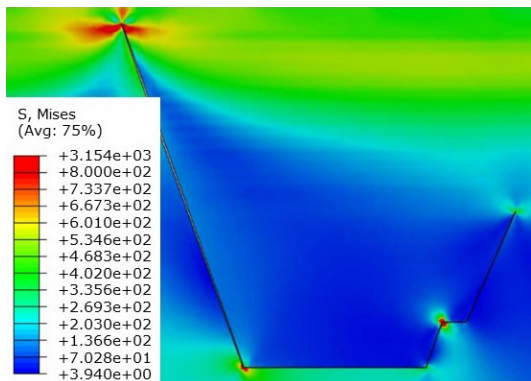
Material	Condition	Number of cycles to spallation
Steel	Case-hardened	8.59e7
Steel	Coated	3.89e6
Titanium	Coated	6.71e6

Table 6 Experimental RCF tests: results, adapted from [19]

	Case-hardened		WC/C coated	
Number of cycles	100,000	150,000	100,000	150,000
A_d [μm²]	1,352	1,561	319	330
d_d [μm]	3.0	4.0	1.3	2.0
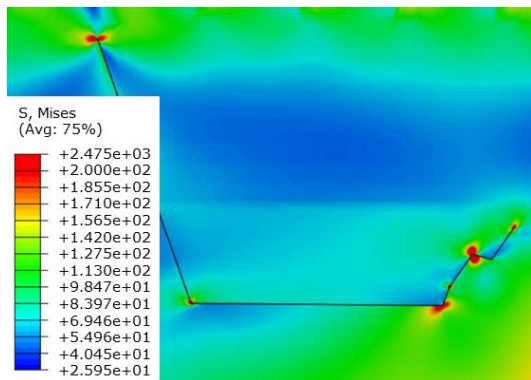
(a)

(b)
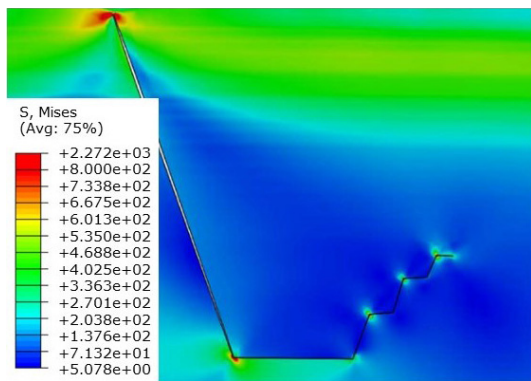
(c)

Fig. 7 FEM analysis for RCF: final stage of crack propagation:
(a) case-hardened steel; (b) coated steel; (c) coated titanium,
adapted from [18]

section A_d and maximum damage depth d_d at the middle of the tooth thickness in lubricated conditions are reported in Table 6 [19].

4 Discussion

4.1 FE analysis for tooth root fatigue

Regarding tooth root fatigue, depositing surface coatings could be an alternative to case-hardening even though it is not so effective. In detail, the number of cycles shown in Table 4 reveals that the application of a coating on a steel substrate tends to postpone crack propagation compared to uncoated, non-case-hardened steel, thanks to the high compressive residual stresses induced by the deposition process. The surface residual stresses are equal to −2,500 MPa. The enhancement in the fatigue limit induced by the coating deposition is highlighted also in [32]. However, the fatigue strength of the case-hardened steel is the best performance obtained, since case-hardening induces much lower stresses on a deeper layer of material.

It has to be stressed that the stress intensity factor range is not constant during propagation. This variation could not be considered in the adopted model, which was discrete. An average between the stress intensity factor range for the initial and for the final crack depth was calculated.

By comparing the results for the coated steel and coated titanium spur gears, in terms of number of cycles needed for the crack growth from 100 μm to 200 μm, a lower crack propagation rate can be observed for the spur gears in titanium: 432,220 cycles are needed for the Ti6Al4V gears and 104,184 for those in 15NiCr13. The stress intensity factor range is related to Young's modulus of the bulk material, which is 113 GPa for titanium and 206 GPa for steel. The higher the stress intensity factor range, the higher the propagation rate and therefore the lower the number of cycles required to reach a certain crack depth.

Hence the fatigue life of coated Ti6Al4V gears is longer than the fatigue life of the coated 15NiCr13 gears and is analogous to the one provided by case-hardened steel [17].

4.2 FEM analysis for RCF

In all the cases presented of FEM analysis for RCF, the crack propagated both from the top and from the rear crack tips with an initial pure Mode II propagation and a subsequent mixed mode, with prevalence of Mode II.

As regards the number of cycles to final spallation, the case-hardened steel gear showed a significant increment

in cycles compared to the coated, non-case-hardened steel gear and the titanium-coated gear, Table 5. The coated titanium gears guarantee a longer fatigue life than the coated steel ones, with a 72% increase in performance. As seen in Section 4.1, the low crack propagation rate obtained for the titanium gears is motivated by the low Young's modulus of the bulk material. In addition, the higher friction coefficient of titanium may have played a role since the initial propagation mode was found to be Mode II. The best performance of the case-hardened spur gear is again due to the high penetration depth of the residual stresses induced by the treatment [18]. The deposition of a coating with a high influence depth could be a powerful solution and also the combined action of coating deposition and case-hardening could be investigated.

For both loading cases analyzed in this paper, fatigue and RCF, the Author underlines the importance of obtaining a coherent residual stress distribution that can be implemented in the FE model. FE modelling can be used to optimize the variables affecting the fatigue and RCF behavior of coated gears [33].

4.3 Experimental RCF tests

The results of the RCF tests summarized in Table 6 clearly point out that the deposition of the WC/C coating significantly reduces the amount of material removed after 100,000 and 150,000 cycles and the maximum damage depth, thus improving the performance of the case-hardened gears. Lubrication plays a key role in maintaining the adhesion of the WC/C film, which has proven to be easily damaged or delaminated without lubricating oil [19].

5 Conclusions

This paper summarizes the FE analyses and experimental tests to evaluate the effects of the bulk material and the surface treatment on the fatigue and RCF behaviors of spur gears. The procedure allows to identify the best solution.

The tooth root fatigue behavior of non-case-hardened, case-hardened and CrN coated 15NiCr11 steel gears, and TiN coated Ti6Al4V titanium gears has been studied. The outcomes show that the best performance is obtained by the classical case-hardened steel spur gear thanks to the residual stress field induced by the treatment, which covers a very thick layer of the spur gear. However, the deposition of TiN on Ti6Al4V can retardate the crack propagation.

The same results have been obtained in the RCF simulation, considering WC/C coated and uncoated case-hardened 16NiCr11 steel: the WC/C coated steel performs better than the uncoated, non-case-hardened steel, while the case-hardened material has the best performance. Coated Ti6Al4V has shown better performance than the coated, non-case-hardened steel, suggesting a possible application of titanium alloys in high-performance spur gears.

RCF experiments revealed a marked improvement in the tooth surface performance for the spur gears coated with WC/C in lubricated conditions, in terms of removal of material and maximum damage depth reduction.

Acknowledgments

References

[1]   Baragetti, S., Gelfi, M., La Vecchia, G. M., Lecis, N. "Fatigue resistance of CrN thin films deposited by arc evaporation process on H11 tool steel and 2205 duplex stainless steel", Fatigue & Fracture Engineering Materials & Structures, 28(7), pp. 615–621, 2005.
https://doi.org/10.1111/j.1460-2695.2005.00905.x

[2]   Goward, G. W. "Progress in coatings for gas turbine airfoils", Surface and Coatings Technology, 108–109, pp. 73–79, 1998.
https://doi.org/10.1016/S0257-8972(98)00667-7

[3]   Love, C. A., Cook, R. B., Harvey, T. J., Dearnley, P. A., Wood, R. J. K. "Diamond like carbon coatings for potential application in biological implants—a review", Tribology International, 63, pp. 141–150, 2013.
https://doi.org/10.1016/j.triboint.2012.09.006

[4]   Bobzin, K., Bagcivan, N., Goebbels, N., Yilmaz K., Hoehn, B.-R., Michaelis, K., Hochmann, M. "Lubricated PVD CrAlN and WC/C coatings for automotive applications", Surface and Coatings Technology, 204(6–7), pp. 1097–1101, 2009.
https://doi.org/10.1016/j.surfcoat.2009.07.045

[5]   Zellner, M. B., Chen, J. G. "Surface science and electrochemical studies of WC and W_2C PVD films as potential electrocatalysts", Catalysis Today, 99(3–4), pp. 299–307, 2005.
https://doi.org/10.1016/j.cattod.2004.10.004

[6]   Baragetti, S., La Vecchia, G. M., Terranova, A. "Variables affecting the fatigue resistance of PVD-coated components", International Journal of Fatigue, 27(10–12), pp. 1541–1550, 2005.
https://doi.org/10.1016/j.ijfatigue.2005.06.011

[7]   Puchi-Cabrera, E. S., Staia, M. H., Lesage, J., Gil, L., Villalobos-Gutiérrez, C., La Barbera-Sosa, J., Ochoa-Pérez, E. A., Le Bourhis, E. "Fatigue behavior of AA7075-T6 aluminum alloy coated with ZrN by PVD", International Journal of Fatigue 2008, 30(7), pp. 1220–1230.
https://doi.org/10.1016/j.ijfatigue.2007.09.001

[8]   Baragetti, S., Gerosa, R., Villa, F. "Fatigue behaviour of thin coated Al 7075 alloy with low temperature PVD coatings", Key Engineering Materials, 577–578, pp. 221–224, 2013.
https://doi.org/10.4028/www.scientific.net/KEM.577-578.221

[9] Baragetti, S., Borzini, E., Božic, Ž., Arcieri, E. V. "On the fatigue strength of uncoated and DLC coated 7075-T6 aluminum alloy", Engineering Failure Analysis, 102, pp. 219–225, 2019.
https://doi.org/10.1016/j.engfailanal.2019.04.035

[10] Arcieri, E. V., Baragetti, S., Borzini, E. "Bending fatigue behavior of 7075-aluminum alloy", Key Engineering Materials, 774, pp. 1–6, 2018.
https://doi.org/10.4028/www.scientific.net/KEM.774.1

[11] Baragetti, S., Božic, Ž., Arcieri, E. V. "Stress and fracture surface analysis of uncoated and coated 7075-T6 specimens under the rotating bending fatigue loading", Engineering Failure Analysis, 112, 104512, 2020.
https://doi.org/10.1016/j.engfailanal.2020.104512

[12] Baragetti, S., Arcieri, E. V. "Effects of thin hard film deposition on fatigue strength of AA7075-T6", Proceedings of the Institution of Mechanical Engineers, Part C: Journal of Mechanical Engineering Science, 2020.
https://doi.org/10.1177/0954406220980505

[13] Baragetti, S., Terranova, A. Tordini, F. "Contact Fatigue Behaviour of PVD-Coated Spur Gears", Key Engineering Materials, 385–387, pp. 57–60, 2008.
https://doi.org/10.4028/www.scientific.net/KEM.385-387.57

[14] Saini, B. S., Gupta, V. K. "Effect of WC/C PVD coating on fatigue behaviour of case carburized SAE8620 steel", Surface and Coatings Technology, 205(2), pp. 511–518, 2010.
https://doi.org/10.1016/j.surfcoat.2010.07.022

[15] Puchi-Cabrera, E. S., Staia, M. H., Ochoa-Pérez, E. A., Teer, D. G., Santana-Méndez, T. T., La Barbera-Sosa, J. G., Chicot, D., Lesage, J. "Fatigue behavior of a 316L stainless steel coated with a DLC film deposited by PVD magnetron sputter ion plating", Materials Science and Engineering: A, 527(3), pp. 498–508, 2010.
https://doi.org/10.1016/j.msea.2009.09.030

[16] Kumar, K., Arul, S. "Investigation of mechanical properties on nano cuprous oxide coated/uncoated spur gear", IOP Conference Series: Materials Science and Engineering, 954, 012023, 2020.
https://doi.org/10.1088/1757-899X/954/1/012023

[17] Baragetti, S. "Fatigue resistance of steel and titanium PVD coated spur gears", International Journal of Fatigue, 29(9–11), pp. 1893–1903, 2007.
https://doi.org/10.1016/j.ijfatigue.2006.11.005

[18] Baragetti, S., Cavalleri, S., Tordini, F. "A Numerical and Experimental Study of the RCF Behaviour of PVD-coated Spur Gears", Key Engineering Materials, 452–453, pp. 589–592, 2010.
https://doi.org/10.4028/www.scientific.net/KEM.452-453.589

[19] Baragetti, S., Cavalleri, S., Tordini, F. "A Numerical Method to Predict the RCF Behaviour of PVD-coated Transmission Gears and Experimental Results", Procedia Engineering, 10, pp. 1485–1490, 2011.
https://doi.org/10.1016/j.proeng.2011.04.248

[20] Saleem, M., Ashok Raj, J., Shiva Sam Kumar, G., Akhila, R. "Design and analysis of aluminium matrix composite spur gear", Advances in Materials and Processing Technologies, 2020.
https://doi.org/10.1080/2374068X.2020.1814983

[21] Czinege, I. "Mass Optimization of Gears", Periodica Polytechnica Mechanical Engineering, 63(2), pp. 75–79, 2019.
https://doi.org/10.3311/PPme.11648

[22] Zhang, Y., Purssell, C., Mao, K., Leigh, S. "A physical investigation of wear and thermal characteristics of 3D printed nylon spur gears", Tribology International, 141, 105953, 2020.
https://doi.org/10.1016/j.triboint.2019.105953

[23] Baragetti, S., Borzini, E., Arcieri, E. V. "Effects of environment and stress concentration factor on Ti-6Al-4V specimens subjected to quasi-static loading", Procedia Structural Integrity, 12, pp. 173–182, 2018.
https://doi.org/10.1016/j.prostr.2018.11.097

[24] Paracchini, L., Cavallotti, P. "Manuale di trattamenti e finiture" (Handbook of treatments and finishes), Tecniche Nuove, 2003. ISBN 978-88-481-1405-9 (in Italian)

[25] Milella, P. P. "Fatigue and Corrosion in Metals", Springer, 2013. ISBN 978-88-470-2335-2
https://doi.org/10.1007/978-88-470-2336-9

[26] Paris, P., Erdogan, F. "A critical analysis of crack propagation laws", Journal of Basic Engineering, 85(4), pp. 528–534, 1963.
https://doi.org/10.1115/1.3656900

[27] El Haddad, M. H., Smith, K. N., Topper T. H. "Fatigue crack propagation of short cracks", Journal of Engineering Materials and Technology, 101(1), pp. 42–46, 1979.
https://doi.org/10.1115/1.3443647

[28] Miller, K. J. "The short crack problem", Fatigue & Fracture Engineering Materials & Structures, 5(3), pp. 223–232, 1982.
https://doi.org/10.1111/j.1460-2695.1982.tb01250.x

[29] Murakami, Y., Endo, M. "Effects of defects, inclusions and inhomogeneities on fatigue strength", International Journal of Fatigue, 16(3), pp. 163–182, 1994.
https://doi.org/10.1016/0142-1123(94)90001-9

[30] Kato, M., Deng, G., Inoue, K., Takatsu, N. "Evaluation of the strength of carburized spur gear teeth based on fracture mechanics", JSME International Journal. Ser. C, Dynamics, control, robotics, design and manufacturing, 36(2), pp. 233–240, 1993.
https://doi.org/10.1299/jsmec1993.36.233

[31] Baragetti, S., Cavalleri, S., Tordini, F. "Contact Fatigue Crack Growth in PVD-Coated Spur Gears", Key Engineering Materials, 417–418, pp. 797–800, 2009.
https://doi.org/10.4028/www.scientific.net/KEM.417-418.797

[32] Baragetti, S., Terranova, A. "Fatigue Resistance of Thin Hard Coated Spur Gears", Structural Durability & Health Monitoring, 1(4), pp. 267–276, 2005.
https://doi.org/10.3970/sdhm.2005.001.267

[33] Baragetti, S., Tordini, F. "A numerical study on the fatigue and rolling contact fatigue behaviour of PVD-coated steel and titanium spur gears", Engineering with Computers, 27(2), pp. 127–137, 2011.
https://doi.org/10.1007/s00366-009-0167-9